Research Square

Preprints are preliminary reports that have not undergone peer review.
They should not be considered conclusive, used to inform clinical practice,
or referenced by the media as validated information.

Biochemical characterization and barrier-disrupting mechanism of TsATG4B, a C54 cysteine protease of Trichinella spiralis, underlying larval intestinal invasion

Yalan Li
Medical College, Henan University of Chinese Medicine
Liqin Chao
Medical College, Henan University of Chinese Medicine
Sihan Liu
Medical College, Henan University of Chinese Medicine
Mengyu Sun
Medical College, Henan University of Chinese Medicine
Baohe Xu
Medical College, Henan University of Chinese Medicine
Qingyuan Hu
Medical College, Henan University of Chinese Medicine
Xiaosa Mu
Medical College, Henan University of Chinese Medicine
Hanyue Zhao
Medical College, Henan University of Chinese Medicine
Shiyi Gao
Medical College, Henan University of Chinese Medicine
Dandan Guo
Medical College, Henan University of Chinese Medicine
Changwei Gu
Tianhao Hongfa Biotechnology Co., Ltd
Zhanjiang Zhang
Medical Plant Garden, Guangxi Zhuang Autonomous Region
Shuying Feng
fsy@hactcm.edu.cn

Medical College, Henan University of Chinese Medicine

Research Article

Keywords: Trichinella spiralis, TsATG4B, cysteine protease, intestinal epithelium, larval invasion

Posted Date: July 27th, 2026

DOI: https://doi.org/10.21203/rs.3.rs-10363990/v1

License: This work is licensed under a Creative Commons Attribution 4.0 International License.
Read Full License

Additional Declarations: No competing interests reported.

Abstract

Trichinellosis is a globally prevalent zoonotic parasitic disease, and cysteine proteases (CPs) secreted by *Trichinella spiralis* are critical virulence effectors that facilitate larval invasion into the host intestinal epithelium. Our previous study identified autophagy-related protease 4B (ATG4B) as a CP potentially involved in larval invasion. However, its detailed enzymatic characteristics and precise invasive mechanism remain unclear. On this basis, the present study systematically characterized the biochemical properties, substrate hydrolysis spectrum, epithelial cytotoxicity, and intestinal tissue binding capacity of recombinant TsATG4B (rTsATG4B). Bioinformatics analysis confirmed that TsATG4B belongs to the C54 peptidase family with conserved catalytic sites Cys113 and His354. The optimal reaction conditions for rTsATG4B were pH 5.5 and 37℃, with *Km* = 60.06 nM and Vmax = 2.391 nM/min. rTsATG4B effectively degraded IgG, hemoglobin and type I collagen, and its enzymatic activity was markedly suppressed by CP-specific inhibitor E-64. *In vitro* immunofluorescence and cell injury assays showed that rTsATG4B time-dependently destroyed tight junction proteins (E-cadherin, claudin-1, occludin) of HT29 epithelial cells and triggered severe morphological damage to primary mouse intestinal epithelial cells. Indirect immunofluorescence test *in vivo* further verified that native TsATG4B specifically bound to intestinal epithelial tissues and aggravated mucosal erosion and villous edema during larval infection. Collectively, these results demonstrate that TsATG4B acts as a functional C54 cysteine protease that promotes *T. spiralis* larval invasion by degrading host structural and immune molecules and disrupting intestinal epithelial barriers. This study elucidates the pathogenic function of TsATG4B and provides experimental evidence for developing novel vaccines or targeted protease inhibitors against trichinellosis.

1. Introduction

Trichinella spiralis (*T. spiralis*) is the causative agent of trichinellosis in humans and animals worldwide [1]. Over the past two decades, this zoonotic pathogen has been documented in 95 (48.5%) countries across the globe; human infections were reported in 47 countries (23.9%), domestic pig transmission in 32 countries (16.3%) and wildlife-associated circulation in 75 countries (38.3%) [2]. Eight trichinellosis outbreaks involving 479 cases and two fatalities were recorded in mainland China from 2009 to 2020, and 7 (87.50%) of these outbreaks originated from consumption of raw or undercooked pork [4].

As an orally transmitted parasitic disease, *T. spiralis* muscle larvae (ML) are released in the intestine and develop into intestinal infectious larvae (IIL) after ingestion [5]. Subsequently, IIL parasitize and embed into intestinal villi and mature into adult worms following four successive molting [6]. Infection causes enteral and parenteral phases including gastrointestinal distress, fever, allergic rash, myalgia, myocarditis, encephalitis, and elevated eosinophils in peripheral blood [7–9]. Small intestinal mucosa constitutes the first-line physical defense against larval colonization, and host-parasite mucosal interactions are essential for subsequent parasitism, yet the detailed invasion mechanism is still unclear. Accumulated evidence shows parasite-derived proteases (serine-, aspartic- and cysteine proteases) dominate larval penetration [10, 11].

Cysteine proteases (CPs) participate in parasite invasion, adhesion, nutrient uptake and immune evasion [11–13]. For example, CPs from *Haemonchus contortus* and *Fasciola hepatica* degrade host extracellular matrix; CPs of *Paragonimus westermani* facilitate excysted metacercarial invasion [16]; CPs from *Plasmodium berghei* and *Plasmodium falciparum* contribute to hepatocyte and erythrocyte entry [17, 18]; *Trichomonas vaginalis* CPs mediate epithelial attachment and mucin breakdown [19]; *Schistosoma mekongi* calpain cleaves fibronectin and complement C3 to escape host innate defense [20], and *Giardia duodenalis* CPs modulate goblet cell function via PAR2 receptor [21]. For another example, in *T. spiralis*, multiple CPs have been validated as core virulence molecules, such as TsCB binds and hydrolyzes type I collagen to assist invasion [22], TsGSCP and another cathepsin B are highly expressed in IIL, localize on larval cuticle and promote epithelial attachment [23, 24], while TsCatL destroys tight junctions to accelerate larval penetration [25]. Our prior work successfully expressed rTsATG4B and confirmed its invasion-promoting function [26], but its enzymatic property and invasive mode remain undefined. Therefore, we systematically analyzed the enzymatic kinetics, substrate preference, *in vitro* epithelial damage and in vivo intestinal binding of TsATG4B to clarify its pathogenic role during trichinellosis.

2. Materials and methods

2.1 Parasites, cell lines and experimental animals

Trichinella spiralis ISS534 strain was originally isolated from naturally infected domestic pigs in Nanyang, China. Primary mouse IECs were isolated from fetal BALB/c mouse small intestine and preserved in our laboratory. C2C12 myoblast and HT29 cell lines were gifted from collaborative labs and preserved routinely. SPF BALB/c and Kunming mice were purchased from Henan Experimental Animal Center. All animal manipulations were approved by the Life Science Ethics Committee of Henan Province (No. DWLL 201903062) and performed in accordance with national laboratory animal welfare guidelines.

2.2 Recombinant TsATG4B production and antiserum preparation

The TsATG4B coding sequence was cloned into pQE-80L and expressed in *E. coli* BL21 cells. Expressed rTsATG4B was purified by Ni-NTA affinity chromatography and subjected to refolding. BALB/c mice were immunized with purified rTsATG4B, and specific antiserum was harvested and quantified via ELISA.

2.3 Bioinformatic and structural prediction

Conserved domain and sequence features were analyzed based on previous data. ORF Finder, NCBI CDD and BLAST were used for sequence retrieval and homology comparison. A total of six homologous CP sequences plus human ATG4A were aligned with TsATG4B using MEGA11, and catalytic sites were determined via multi-alignment against *Ancylostoma ceylanicum* (EPB67082.1). Three-dimensional structure was predicted on the SWISS-MODEL server.

2.4 Determination of enzymatic characteristics

rTsATG4 activity was quantified using AFC fluorescent substrate Ac-KKChaG-AFC (songon bio.com). rTsATG4B was added to the preferred buffers HEPES at the concentration of 12 μg/mL, then was incubated with Ac-KKChaG-AFC at different concentrations (0, 0.001, 0.005, 0.01, 0.05, 0.10, 0.15 and 0.2 μmol) at 37℃. Serial substrate gradients were prepared to calculate K and V according to Michaelis-Menten equation after fluorescence detection on Cytation5 reader (Biotek, USA). Enzymatic activity was determined in pH 2.0–8.0 acetate-phosphate buffer at temperatures ranging from 25℃ to 65℃, and fluorescence signals were recorded every 10 min within 90 min. Using the E-64 (trans-epoxysuccinyl-l-leucylamido- (4-guanidino) butane, the CP specific inhibitor) as an inhibitor, rTsATG4B activity was determined. Purified rTsATG4B was pre-incubated with equal volume of E-64 (final 1:1 v/v) at 37℃, and substrate hydrolysis was detected at set intervals of 10 min, in which the untreated rTsATG4B served as blank control. All assays were conducted in triplicate in black 96-well plates.

2.5 Proteolytic degradation of host-derived proteins

Purified rTsATG4B (1, 2, 3 μg) was incubated with 5 μg of human IgG (Sigma), goat IgG (Solarbio, Beijing, China), mouse hemoglobin or rat tail collagen I (Solarbio, Beijing, China) respectively at 37℃ for 12 h, and digestion products were separated by SDS-PAGE and stained with Coomassie blue.

2.6 *In vitro* epithelial damage assay

Confluent HT29 grown on coverslips were treated with 12 μg/mL rTsATG4B for 10, 90 or 120 min. After fixation and blocking, samples were incubated with primary antibodies against E-cadherin, claudin-1 and occludin, followed by corresponding fluorescent secondary antibodies (dilution 1:200) including Dylight 405-conjugated goat anti-rat IgG (blue-fluorescence staining), Alex Fluor 555-conjugated goat anti-rabbit IgG (red-fluorescence staining), and FITC-conjugated goat anti-mouse (green-fluorescence staining) at 37℃ for 1 h before microscopic observation. IEC and C2C12 monolayers were treated with rTsATG4, papain or PBS (blank). For inhibition group, rTsATG4 was pre-treated with 10 μM E-64 for 30 min before cell incubation, and cellular changes were recorded by microplate reader Cytation 5 (USA Biotek).

2.7 IIFT detection of TsATG4B binding property to intestine

To investigate the binding force of natural TsATG4B to intestine epithelium, uninfected mouse small intestine and liver paraffin sections were prepared. After being fixed in 4% paraformaldehyde and embedded in paraffin, anti-rTsATG4B serum, infection serum and preimmune serum were used as primary antibody, FITC/Cy3-labeled secondary antibody and PI nuclear counterstain tissues were used to perform the IIFT assay *in vitro* as reported previously[27]. For *in vivo* localization, intestines collected at 2, 6, 8, 12 h post-infection (hpi) and infected mouse diaphragm (42 dpi) as the control group.were processed identically.

3. Results

3.1 Bioinformatics analysis

BLAST comparison revealed high sequence homology between TsATG4 and ATG family CPs from *T. nelsoni*, *Ancylostoma ceylanicum*, *Schistosoma haematobium*, *Saccharomyces cerevisiae*, *human* and *Trypanosoma cruzi*. Multiple sequence alignment identified conserved catalytic Cys113 and His354 within the C54 peptidase domain (Fig. 1). SWISS-MODEL structural simulation showed the protein contained 31.88% α-helix, 3.62% β-sheet and 51.45% random coil; predicted catalytic residues were exposed on protein surface (Fig. 2). Ramachandran plot showed over 88% residues fell in allowed regions, indicating reliable structural modeling.

3.2 Enzymatic kinetic results

Fluorescence intensity displayed good linear correlation with AFC concentration (R^2=0.955). The calculated kinetic constants were K□=60.06 nM, V□□□=2.391 nM/min (Fig. 3). Maximal enzymatic activity occurred at pH 5.5 and 37℃ (Fig. 4). Pre-incubation with E-64 significantly suppressed substrate hydrolysis, and fluorescence plateaued at 60 min in untreated group (Fig. 5).

3.3 Proteolysis of host macromolecules

SDS-PAGE results demonstrated dose-dependent degradation of human IgG, goat IgG, mouse hemoglobin and rat tail type I collagen along with increasing rTsATG4 dosage in pH 5.5 solution buffer at 37℃. Target bands faded or disappeared with elevated protease amount (1–3 μg) (Fig. 6A-D). The gradually fading stripes and the disappearance of 25 kDa protein bands indicated that rTsATG4B could hydrolyze the mouse Hb (Fig. 6C). In Fig. 6D, the absence of protein bands more than 150 kDa in size indicates that collagen I rat tail type I is digested.

3.4 *In vitro* cellular injury

3.4.1 IEC morphological lesion

After rTsATG4 incubation with IEC monolayer, cell-cell connections were disrupted and a focalized damage of monolayer continuity was lost (Fig. 7A). Through co-culture of 30–60 min, the number of damaged IEC cells was increased, and a large number of blebs emerged at the time of 120 min, which revealed that rTsATG4B protein induced time-dependent effects on the surface of IEC monolayer (Fig. 7B-D). No visible damage was observed in papain-treated IEC, rTsATG4-treated C2C12 or PBS control groups. And the E-64 pre-incubation fully abolished cell damage (Fig. 7E-H).

3.4.2 Disruption of cell junction proteins

Immunofluorescence showed E-cadherin, claudin-1 and occludin localized at cell borders in untreated HT29. The integrity of HT29 cells and cellular junctions were not obvious within 10 min. With prolonged rTsATG stimulation, junction fluorescence gradually decreased, and the cells aggregated and separated after 90–120 min incubation (Fig. 8).

3.5 *In vivo* intestinal binding and mucosal injury

IIFT confirmed the specific binding of exogenous rTsATG4 to normal mouse intestinal epithelium (Fig. 9). In infected intestinal samples, positive red fluorescence co-localized with edematous, disorganized and eroded villi with prolonged infection, whereas diaphragm tissue only exhibited DAPI nuclear staining without specific red signal (Fig. 10).

4. Discussion

Cysteine proteases are grouped into multiple clans, and most parasitic CPs belong to CA superfamily including C1 (cathepsin B/L-like) and C2 (calpain-like) subfamilies [12, 28]. Cumulative evidence proves *T. spiralis*-derived CPs function as important virulence effectors facilitating epithelial degradation and larval colonization [10, 29, 30]. Consistenting with previous preliminary data [26], the present study systematically characterized the biochemical features and pathogenic function of TsATG4B. Bioinformatic prediction confirmed TsATG4 is a canonical C54 CP with exposed conserved catalytic residues, which supported its intrinsic proteolytic capacity. Its optimal pH and temperature matched gastrointestinal microenvironment conditions, consistent with biochemical features of numerous parasite-derived CPs [31–34]. Low K□ value reflected high substrate affinity typical for virulence-associated proteases [35, 36], and complete activity block by the CP-specific inhibitor E-64 further verified its CP property [12].

Substrate tests proved rTsATG4 efficiently digested IgG, hemoglobin and collagen I-key host proteins involved in immunity, nutrient supply, and tissue structure. IgG degradation suggests that TsATG4B may help the parasite evade host humoral immunity, while hemoglobin hydrolysis supports nutrient acquisition during larval development. Collagen degradation directly contributes to extracellular matrix (ECM) breakdown, enabling larvae to penetrate the intestinal wall. These findings imply that TsATG4B promotes immune evasion and ECM degradation to facilitate larval nutrient acquisition and tissue penetration, consistent with previously reported functions of CPs in multiple helminth species [22, 37–40]. The intestinal epithelium serves as the primary physical barrier against pathogen invasion, with tight junctions (TJs) and adherens junctions (AJs) maintaining barrier integrity [10, 40–44]. Furthermore, the IECs serves as the fundamental and primary physical barrier to protect against pathogens, toxins and harmful substances in the intestinal cavity[41–42]. *In vitro* experiments verified rTsATG4 induced time-dependent tight junction degradation and exclusive damage on IEC rather than C2C12 cells, and E-64 completely abrogated injury, confirming damage relies on its protease activity.

In vivo IIFT assays further validated that TsATG4B specifically binds to mouse intestinal epithelium and accumulates at larval invasion sites. During infection, TsATG4B colocalizes with damaged villi that exhibited progressive edema, disorganization, and erosion over time, supporting that TsATG4B contributes to intestinal mucosal injury during larval invasion, consistent with our *in vitro* data. Similar to our findings, cysteine proteases secreted by various intestinal parasites act as crucial virulence factors that disrupt the host mucosal barrier and facilitate parasitic invasion. For instance, *Schistosoma*

mansoni-derived cathepsin B exhibits potent tissue-degrading capacity to support parasite migration [49], and the homologous Ac-cathB-2 of *Angiostrongylus cantonensis* mediates larval penetration across the rat intestinal wall [50]. In protozoan parasites, CPs from *Giardia duodenalis* degrade goblet cell mucins and impair the intestinal mucus barrier, whereas giardipain-1 elevates epithelial permeability, triggers apoptosis, and causes villous destruction, epithelial exfoliation, and goblet cell edema in infected animals [51, 52]. In *Entamoeba histolytica*, CPs with ICE-like activity stimulate the production of pro-inflammatory IL-1β and IL-8 to initiate intestinal inflammation and mucosal damage [53]. In line with these findings, studies on *T. spiralis* proteases further support our conclusion: neutralizing antibodies against TsSPc form cap-like immune complexes at the larval anterior and suppress invasion, and anti-TsGSCP and anti-TsSPI antibodies exert similar invasion-blocking effects [24, 54–57]. Collectively, these findings support that TsATG4B acts as an important pathogenic protease contributing to intestinal mucosal damage during *T. spiralis* larval infection.

In vivo IIFT validated TsATG4B accumulates at invasion loci and co-localizes with injured villi, which coincided with *in vitro* findings. Published literatures also confirmed CPs from various intestinal parasites damage mucosal barrier to promote infection: *Schistosoma mansoni* cathepsin B degrades host tissue matrix [49]; *Angiostrongylus cantonensis* Ac-cathB-2 facilitates intestinal penetration [50]; *Giardia duodenalis* CPs degrade goblet cell mucins and trigger epithelial apoptosis via Giardipain-1 [51, 52]; *Entamoeba histolytica* CPs drive proinflammatory cytokine release and mucosal inflammation [53]. In *T. spiralis*, neutralizing antibody against TsSPc, TsGSCP and TsSPI form surface cap complexes and inhibit larval invasion [24, 54–57]. Collectively, these references strongly support that TsATG4B acts as a pathogenic cysteine protease to trigger intestinal mucosal damage during larval infection.

In summary, TsATG4B is an important virulence factor of *T. spiralis*. Biochemical enzymatic characterization confirmed that recombinant TsATG4B exhibits typical cysteine protease activity with optimal catalytic conditions at pH 5.5 and 37℃, a low Km value of 60.06 nM reflecting high substrate affinity, and its proteolytic activity was completely abolished by the cysteine protease-specific inhibitor E-64. As a high-efficiency C54 cysteine protease, it degrades host immune and structural proteins (IgG, hemoglobin and type I collagen), disrupts epithelial tight junctions and induces intestinal damage to favor larval parasitism. This study deepens our understanding of trichinellosis pathogenesis and provides a promising molecular target for anti-parasite vaccine and inhibitor development.

Abbreviations

T. spiralis
Trichinella spiralis
CP
cysteine protease
ML
muscle larvae
IIL

intestinal infective larvae
NBL
newborn larvae
IEC
intestinal epithelial cell
rTsATG4B
recombinant *T. spiralis* ATG4B
AFC
7-amino-4-trifluoromethyl coumarin
E-64
trans-epoxysuccinyl-l-leucylamido- (4-guanidino) butane
IIFT
indirect immunofluorescence test
SD
standard deviation
SPF
specific-pathogen-free

Declarations

Ethics approval and consent to participate

All animal experiments were approved by the Life Science Ethics Committee of Henan Province (No. DWLL 201903062).

Competing interests

The authors declare no competing interests.

Funding

The authors thank the organizations for their funding support: The Joint Funds of Science and Technology Research and Development Project of Henan Province (No. 232301420070, 235200810108), Key Research and Development Special Project of Henan Province (241111311200), and the Basic Research Project of the Key Research Project Plan of Henan Provincial Universities (23ZX005), Doctoral Research Fund of Henan University of Chinese Medicine(BSJJ2022-07), Project Approval for the Scientific Research Nursery Construction of Henan University of Chinese Medicine(2025MPXS22).

Author Contribution

All authors participated in manuscript drafting, revision and final approval. Yalan Li, Liqin Chao and Sihan Liu performed original manuscript writing; Mengyu Sun, Baohe Xu, Qingyuan Hu and Xiaosa Mu completed figure preparation; Hanyue Zhao and Shiyi Gao collected relevant literatures; animal experiments were finished by Yalan Li, Liqin Chao and Sihan Liu; cell experiments were conducted by Baohe Xu, Dandan Guo and Qingyuan Hu; Changwei Gu and Zhanjiang Zhang managed statistical collation. Shuying Feng supervised the whole research and critically revised the manuscript. All authors have read and agreed on the final version.

References

1. Murakami M, Tokiwa T, Sugiyama H, Shiroyama M, Morishima Y, Watanabe S, Sasamori T, Kondo M, Mano T, Tsuruga H (2023) *Trichinella* T9 in wild bears in Japan: Prevalence, species/genotype identification, and public health implications. Int J Parasitol Parasites Wildl 21:264–268
2. Borhani M, Fathi S, Harandi MF, Simsek S, Ahmed H, Wu X, Liu M (2023) *Trichinella* infections in animals and humans of Iran and Turkey. Front Med 10:1088507
3. Intirach J, Shu C, Lv X, Gao S, Sutthanont N, Chen T, Lv Z (2024) Human parasitic infections of the class Adenophorea: global epidemiology, pathogenesis, prevention and control. Infect Dis Poverty 13:48
4. Zhang XZ, Wang ZQ, Cui J (2022) Epidemiology of trichinellosis in the People's Republic of China during 2009–2020. Acta Trop 229:106388
5. Ma KN, Zhang Y, Zhang ZY, Wang BN, Song YY, Han LL, Zhang XZ, Long SR, Cui J, Wang ZQ (2023) *Trichinella spiralis* galectin binding to toll-like receptor 4 induces intestinal inflammation and mediates larval invasion of gut mucosa. Vet Res 54:113
6. Ren HN, Bai SJ, Wang Z, Han LL, Yan SW, Jiang P, Zhang X, Wang ZQ, Cui J (2021) A metalloproteinase Tsdpy31 from *Trichinella spiralis* participates in larval molting and development. Int J Biol Macromol 192:883–894
7. Ribicich M, Gamble HR, Bolpe J, Scialfa E, Krivokapich S, Cardillo N, Betti A, Holzmann ML, Pasqualetti M, Fariña F, Rosa A (2010) *Trichinella* infection in wild animals from endemic regions of Argentina. Parasitol Res 107:377–380
8. Elgendy WMA, Othman AA, Soliman NA, Baiomy N, El-Guindy DM, Elgendy DI (2025) Immunomodulatory and anti-inflammatory effects of fluvoxamine during the intestinal phase of *Trichinella spiralis* infection in mice. Parasitol Res 124:112
9. Kompoura V, Karapantzou I, Mitropoulou G, Parisis NA, Gkalpinos VK, Anagnostou VA, Tsiailanis AD, Vasdekis EP, Koutsaliaris IK, Tsouka AN, Karapetsi L, Madesis P, Letsiou S, Florou D, Koukkou AI, Barbouti A, Tselepis AD, Kourkoutas Y, Tzakos AG (2023) Exploiting the beneficial effects of *Salvia officinalis* L. extracts in human health and assessing their activity as potent functional regulators of food microbiota. Food Chem 441:138175
10. Song YY, Lu QQ, Han LL, Yan SW, Zhang XZ, Liu RD, Long SR, Cui J, Wang ZQ (2022) Proteases secreted by *Trichinella spiralis* intestinal infective larvae damage the junctions of the intestinal

epithelial cell monolayer and mediate larval invasion. Vet Res 53:19

11. Yang N, Matthew MA, Yao C (2023) Roles of cysteine proteases in biology and pathogenesis of parasites. Microorganisms 11:1397
12. Song YY, Wang LA, Ren HN, Qi X, Sun GG, Liu RD, Jiang P, Zhang X, Cui J, Wang ZQ (2018) Cloning, expression and characterisation of a cysteine protease from *Trichinella spiralis*. Folia Parasitol 65:007
13. Argüello-García R, Carrero JC, Ortega-Pierres MG (2023) Extracellular cysteine proteases of key intestinal protozoan pathogens-factors linked to virulence and pathogenicity. Int J Mol Sci 24:12850
14. Gamble HR, Mansfield LS (1996) Characterization of excretory-secretory products from larval stages of *Haemonchus contortus* cultured in vitro. Vet Parasitol 62:291–305
15. Cwiklinski K, Jewhurst H, McVeigh P, Barbour T, Maule AG, Tort J, O'Neill SM, Robinson MW, Donnelly S, Dalton JP (2018) Infection by the helminth parasite *Fasciola hepatica* requires rapid regulation of metabolic, virulence, and invasive factors to adjust to its mammalian host. Mol Cell Proteom 17:792–809
16. Na BK, Kim SH, Lee EG, Kim TS, Bae YA, Kang I, Yu JR, Sohn WM, Cho SY, Kong Y (2006) Critical roles for excretory-secretory cysteine proteases during tissue invasion of *Paragonimus westermani* newly excysted metacercariae. Cell Microbiol 8:1034–1046
17. Bzik DJ, Li WB, Horii T, Inselburg J (1987) Molecular cloning and sequence analysis of the *Plasmodium falciparum* dihydrofolate reductase-thymidylate synthase gene. Proc Natl Acad Sci U S A 84:8360–8364
18. Briones MR, Tsuji M, Nussenzweig V (1996) The large difference in infectivity for mice of *Plasmodium berghei* and *Plasmodium yoelii* sporozoites cannot be correlated with their ability to enter into hepatocytes. Mol Biochem Parasitol 77:7–17
19. Hernández HM, Marcet R, Sarracent J (2014) Biological roles of cysteine proteinases in the pathogenesis of *Trichomonas vaginalis*. Parasite 21:54
20. Chaimon S, Limpanont Y, Reamtong O, Ampawong S, Phuphisut O, Chusongsang P, Ruangsittichai J, Boonyuen U, Watthanakulpanich D, O'Donoghue AJ, Caffrey CR, Adisakwattana P (2019) Molecular characterization and functional analysis of the *Schistosoma mekongi* Ca^{2+}-dependent cysteine protease (calpain). Parasit Vectors 12:383
21. Fekete E, Allain T, Amat CB, Mihara K, Saifeddine M, Hollenberg MD, Chadee K, Buret AG (2022) *Giardia duodenalis* cysteine proteases cleave proteinase-activated receptor-2 to regulate intestinal goblet cell mucin gene expression. Int J Parasitol 52:285–292
22. Zhao YJ, Cheng G, Feng MM, Wang YX, Zhang ZF, Zhang X, Jiang P (2024) *Trichinella spiralis* cathepsin B bound and degraded host's intestinal type I collagen. Int J Biol Macromol 257:128728
23. Hu YY, Zhang R, Yan SW, Yue WW, Zhang JH, Liu RD, Long SR, Cui J, Wang ZQ (2021) Characterization of a novel cysteine protease in *Trichinella spiralis* and its role in larval intrusion, development and fecundity. Vet Res 52:113

24. Han Y, Yue X, Hu CX, Liu F, Liu RD, He MM, Long SR, Cui J, Wang ZQ (2020) Interaction of a *Trichinella spiralis* cathepsin B with enterocytes promotes the larval intrusion into the cells. Res Vet Sci 130:110–117
25. Liu RD, Meng XY, Li CL, Lin XZ, Xu QY, Xu H, Long SR, Cui J, Wang ZQ (2023) *Trichinella spiralis* cathepsin L damages the tight junctions of intestinal epithelial cells and mediates larval invasion. PLoS Negl Trop Dis 17:e0011816
26. Li Y, Wang B, Zhu Y, Tian Z, Yang Z, Duan J, Wang Z (2020) The cysteine protease ATG4B of *Trichinella spiralis* promotes larval invasion into the intestine of the host. Vet Res 51:69
27. Hu CX, Xu YXY, Hao HN, Liu RD, Jiang P, Long SR, Wang ZQ, Cui J (2021) Oral vaccination with recombinant *Lactobacillus plantarum* encoding *Trichinella spiralis* inorganic pyrophosphatase elicited a protective immunity in BALB/c mice. PLoS Negl Trop Dis 15:e0009865
28. Barrett AJ, Rawlings ND (2001) Evolutionary lines of cysteine peptidases. Biol Chem 382:727–733
29. Ren HN, Zhuo TX, Bai SJ, Bai Y, Sun XY, Dan Liu R, Long SR, Cui J, Wang ZQ (2021) Proteomic analysis of hydrolytic proteases in excretory/secretory proteins from *Trichinella spiralis* intestinal infective larvae using zymography combined with shotgun LC-MS/MS approach. Acta Trop 216:105825
30. Liu RD, Cui J, Liu XL, Jiang P, Sun GG, Zhang X, Long SR, Wang L, Wang ZQ (2015) Comparative proteomic analysis of surface proteins of *Trichinella spiralis* muscle larvae and intestinal infective larvae. Acta Trop 150:79–86
31. Kianifard L, Yakhchali M, Imani M (2020) The effects of pH and temperature on cysteine protease (Cathepsin B) activity in miracidia and eggs of *Fasciola hepatica*. Iran J Parasitol 15:233–239
32. Lê HG, Kang JM, Võ TC, Yoo WG, Lee KH, Na BK (2022) Biochemical properties of two plasmodium malariae cysteine proteases, Malapain-2 and Malapain-4. Microorganisms 10:193
33. Torralbo-Ramírez V, Molina-Fernández D, Malagón D, Benítez R, Adroher FJ (2019) Differential cleaving of specific substrates for cathepsin-like activity shows cysteine and serine protease activities and a differential profile between *Anisakis simplex* s.s. and *Anisakis pegreffii*, sibling species major etiologic agents of Anisakiasis. Foodborne Pathog Dis 16:744–751
34. Liu RD, Meng XY, Li CL, Long SR, Cui J, Wang ZQ (2022) Molecular characterization and determination of the biochemical properties of cathepsin L of *Trichinella spiralis*. Vet Res 53:48
35. Holm M, Mandava CS, Ehrenberg M, Sanyal S (2019) The mechanism of error induction by the antibiotic viomycin provides insight into the fidelity mechanism of translation. Elife 8:e46124
36. Eisenthal R, Danson MJ, Hough DW (2007) Catalytic efficiency and kcat/KM: a useful comparator? Trends Biotechnol 25:247–249
37. Piao X, Wang Y, Jiang N, Cai P, Duan J, Liu S, Chen Q, Hou N (2025) *Schistosoma japonicum* cathepsin L1: A potential target for anti-schistosomiasis strategies. PLoS Negl Trop Dis 19:e0013241
38. Zhu B, Luo F, Shen Y, Yang W, Sun C, Wang J, Li J, Mo X, Xu B, Zhang X, Li Y, Hu W (2020) *Schistosoma japonicum* cathepsin B2 (SjCB2) facilitates parasite invasion through the skin. PLoS

Negl Trop Dis 14:e0008810

39. Bai H, Cao Y, Chen Y, Zhang L, Wu C, Zhan X, Cheng M (2020) Molecular cloning and characterization of a cathepsin L-like cysteine protease of *Angiostrongylus cantonensis*. Int J Biol Macromol 153:1136–1146
40. Rehman ZU, Deng Q, Umair S, Savoian MS, Knight JS, Pernthaner A, Simpson HV (2016) Excretory/secretory products of adult *Haemonchus contortus* and *Teladorsagia circumcincta* which increase the permeability of Caco-2 cell monolayers are neutralised by antibodies from immune hosts. Vet Parasitol 221:104–110
41. Zeisel MB, Dhawan P, Baumert TF (2019) Tight junction proteins in gastrointestinal and liver disease. Gut 68:547–561
42. Garcia-Hernandez V, Quiros M, Nusrat A (2017) Intestinal epithelial claudins: expression and regulation in homeostasis and inflammation. Ann N Y Acad Sci 1397:66–79
43. Horowitz A, Chanez-Paredes SD, Haest X, Turner JR (2023) Paracellular permeability and tight junction regulation in gut health and disease. Nat Rev Gastroenterol Hepatol 20:417–432
44. Zihni C, Mills C, Matter K, Balda MS (2016) Tight junctions: from simple barriers to multifunctional molecular gates. Nat Rev Mol Cell Biol 17:564–580
45. Pitman RS, Blumberg RS (2000) First line of defense: the role of the intestinal epithelium as an active component of the mucosal immune system. J Gastroenterol 35:805–814
46. Lu QQ, Zhang XZ, Cong PK, Wu JY, Gao TR, Long SR, Liu RD, Wang ZQ, Cui J (2025) A *Trichinella spiralis* serine protease triggers gut epithelial apoptosis and destroys the barrier integrity to mediate larval invasion. PLoS Negl Trop Dis 19:e0013680
47. Cabrera-Licona A, Solano-González E, Fonseca-Liñán R, Bazán-Tejeda ML, Raúl Argüello-García, Bermúdez-Cruz RM, Ortega-Pierres G (2017) Expression and secretion of the *Giardia duodenalis* variant surface protein 9B10A by transfected trophozoites causes damage to epithelial cell monolayers mediated by protease activity. Exp Parasitol 179:49–64
48. Ortega-Pierres G, Argüello-García R, Laredo-Cisneros MS, Fonseca-Linán R, Gómez-Mondragón M, Inzunza-Arroyo R, Flores-Benítez D, Raya-Sandino A, Chavez-Munguía B, Ventura-Gallegos JL, Zentella-Dehesa A, Bermúdez-Cruz RM, González-Mariscal L (2018) Giardipain-1, a protease secreted by *Giardia duodenalis* trophozoites, causes junctional, barrier and apoptotic damage in epithelial cell monolayers. Int J Parasitol 48:621–639
49. Ghoneim H, Klinkert MQ (1995) Biochemical properties of purified cathepsin B from *Schistosoma mansoni*. Int J Parasitol 25:1515–1519
50. Long Y, Cao B, Wang Y, Luo D (2016) Pepsin is a positive regulator of Ac-cathB-2 involved in the rat gut penetration of *Angiostrongylus cantonensis*. Parasit Vectors 9:286
51. Amat CB, Motta JP, Fekete E, Moreau F, Chadee K, Buret AG (2017) Cysteine protease-dependent mucous disruptions and differential mucin gene expression in *Giardia duodenalis* infection. Am J Pathol 187:2486–2498

52. Quezada-Lázaro R, Vázquez-Cobix Y, Fonseca-Liñán R, Nava P, Hernández-Cueto DD, Cedillo-Peláez C, López-Vidal Y, Huerta-Yepez S, Ortega-Pierres MG (2022) The cysteine protease Giardipain-1 from *Giardia duodenalis* contributes to a disruption of intestinal homeostasis. Int J Mol Sci 23:13649
53. Zhang Z, Wang L, Seydel KB, Li E, Ankri S, Mirelman D, Stanley SL Jr (2000) *Entamoeba histolytica* cysteine proteinases with interleukin-1 beta converting enzyme (ICE) activity cause intestinal inflammation and tissue damage in amoebiasis. Mol Microbiol 37:542–548
54. Sun GG, Ren HN, Liu RD, Song YY, Qi X, Hu CX, Yang F, Jiang P, Zhang X, Wang ZQ, Cui J (2018) Molecular characterization of a putative serine protease from *Trichinella spiralis* and its elicited immune protection. Vet Res 49:59
55. Song YY, Zhang XZ, Wang BN, Weng MM, Zhang ZY, Guo X, Zhang X, Wang ZQ, Cui J (2023) Molecular characterization of a novel serine proteinase from *Trichinella spiralis* and its participation in larval invasion of gut epithelium. PLoS Negl Trop Dis 17:e0011629
56. Guo KX, Bai Y, Ren HN, Sun XY, Song YY, Liu RD, Long SR, Zhang X, Jiang P, Wang ZQ, Cui J (2020) Characterization of a *Trichinella spiralis* aminopeptidase and its participation in invasion, development and fecundity. Vet Res 51:78
57. McVay CS, Bracken P, Gagliardo LF, Appleton J (2000) Antibodies to tyvelose exhibit multiple modes of interference with the epithelial niche of *Trichinella spiralis*. Infect Immun 68:1912–1918

Figures



Figure 1

Bioinformatics analysis and proteolytic activity verification of TsATG4B.

A Multiple sequence alignment of TsATG4B with homologous cysteine proteases from multiple helminths and other organisms (*Ancylostoma ceylanicum*, *Schistosoma haematobium*, *Saccharomyces cerevisiae*, *Homo sapiens*, *and Trypanosoma cruzi*). Conserved catalytic residues Cys113 and His354 are

labeled with pink diamond pattern markers. **B** Schematic domain structure of TsATG4B, showing the conserved C54 peptidase domain and two catalytic active sites Cys113 and His354. **C** Gelatin zymography assay for detecting proteolytic activity of refolded rTsATG4B. Lane M: protein molecular weight marker; Lane 1: refolded rTsATG4B with clear transparent proteolytic bands; Lane 2: heat-denatured rTsATG4B (negative control); Lane 3: rTsATG4B preincubated with cysteine protease inhibitor E-64.

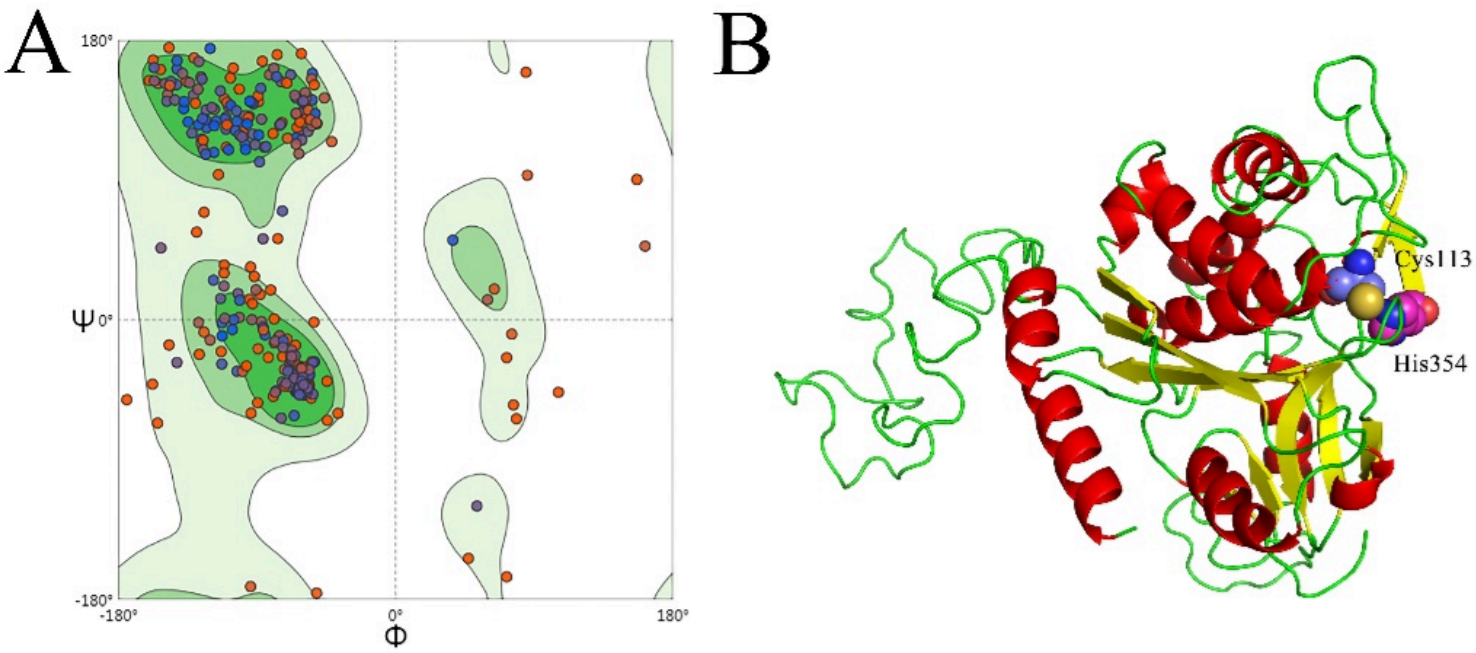


Figure 2

Ramachandran plot and predicted three-dimensional structural model of TsATG4B.

A Ramachandran plot assessment of homology modeling; over 88% of amino acid residues are distributed in favorable allowed regions, indicating reliable structural modeling. **B** SWISS-MODEL predicted 3D structure of TsATG4B: α-helix (red), β-sheet (yellow), random coil (green). Catalytic residues Cys113 (blue sphere) and His354 (magenta sphere) are highlighted on the protein surface.

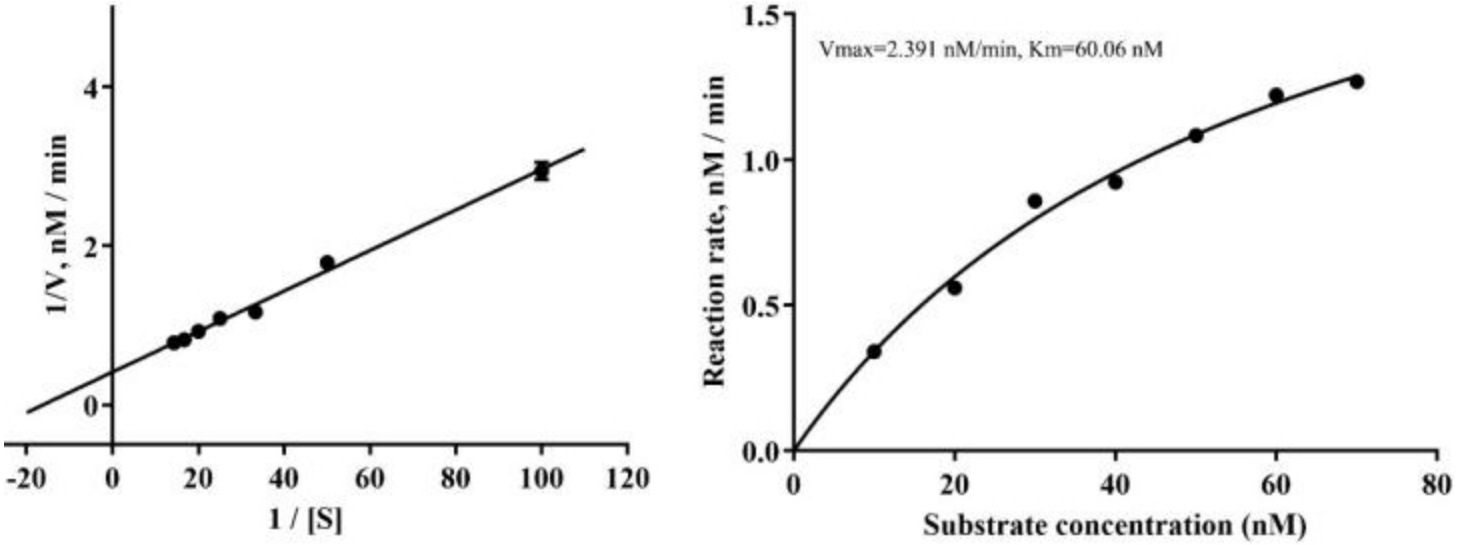


Figure 3

Enzymatic kinetic parameters of rTsATG4B.

A Lineweaver-Burk double-reciprocal plot for calculating Michaelis-Menten constants. **B** Michaelis-Menten kinetic curve of rTsATG4B. All experiments were performed in three biological replicates.

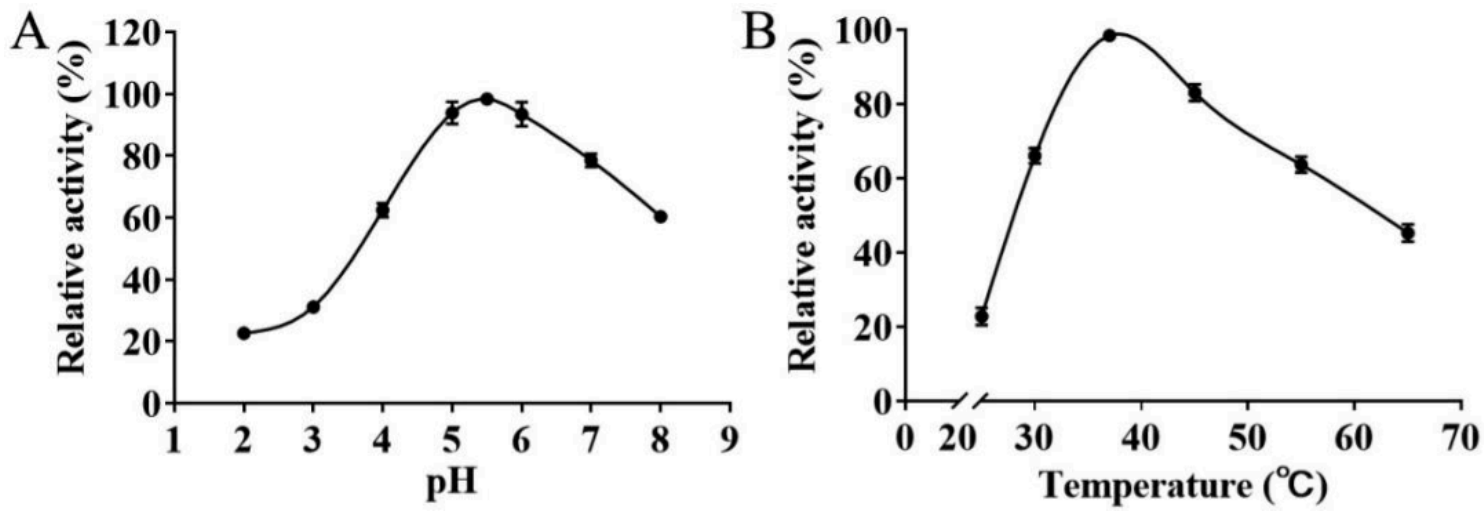


Figure 4

Effects of pH and temperature on the proteolytic activity of rTsATG4B.

A The optimal catalytic pH of rTsATG4B is 5.5 (pH 2.0-8.0). **B** The optimal catalytic temperature is 37℃ (25-65 ℃). All data are presented as Mean±SD.

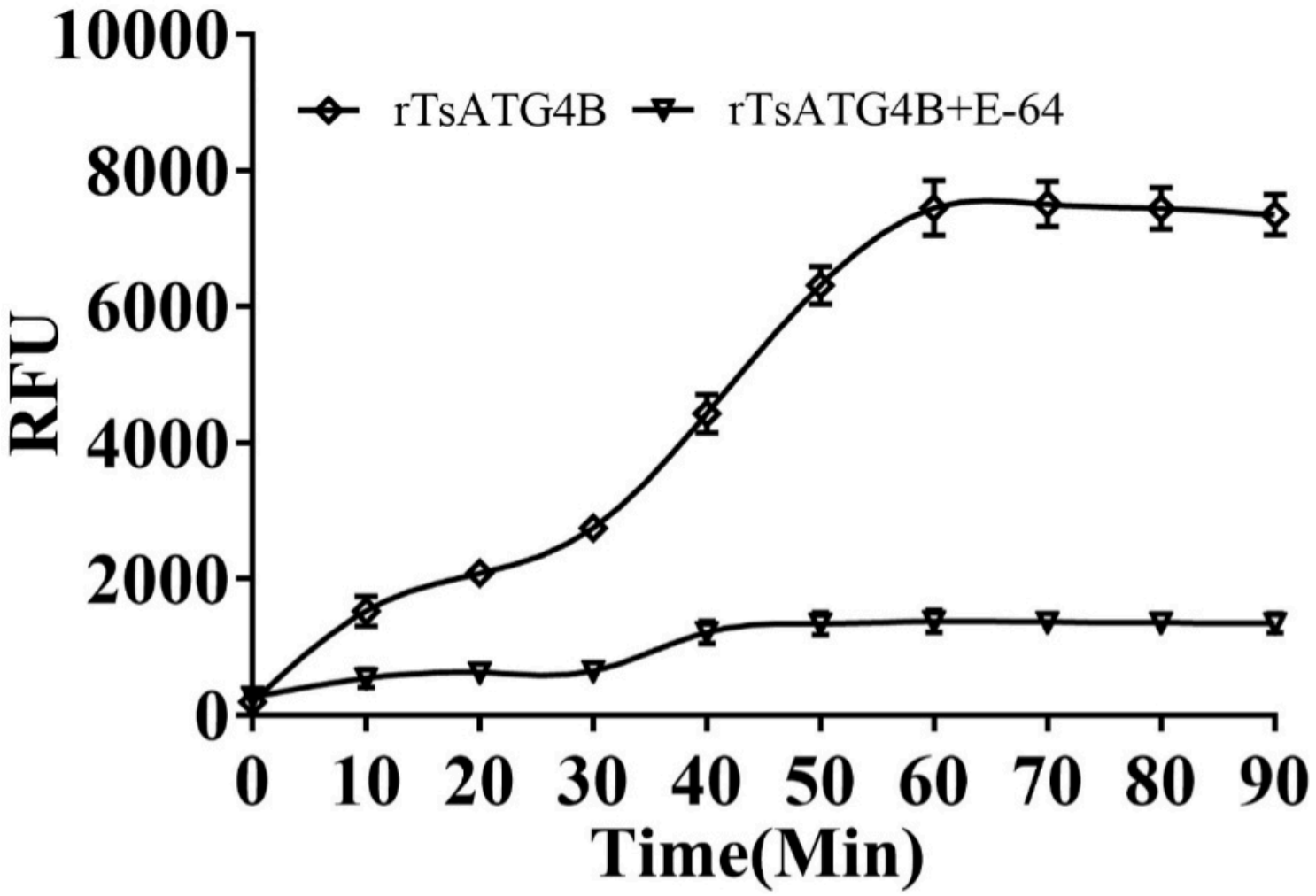


Figure 5

Inhibitory effect of cysteine protease-specific inhibitor E-64 on rTsATG4B activity.

Fluorescence signal (RFU, relative fluorescence unit) released by AFC substrate was detected within 90 min. E-64 preincubation significantly blocked the proteolytic activity of rTsATG4B (Mean±SD).

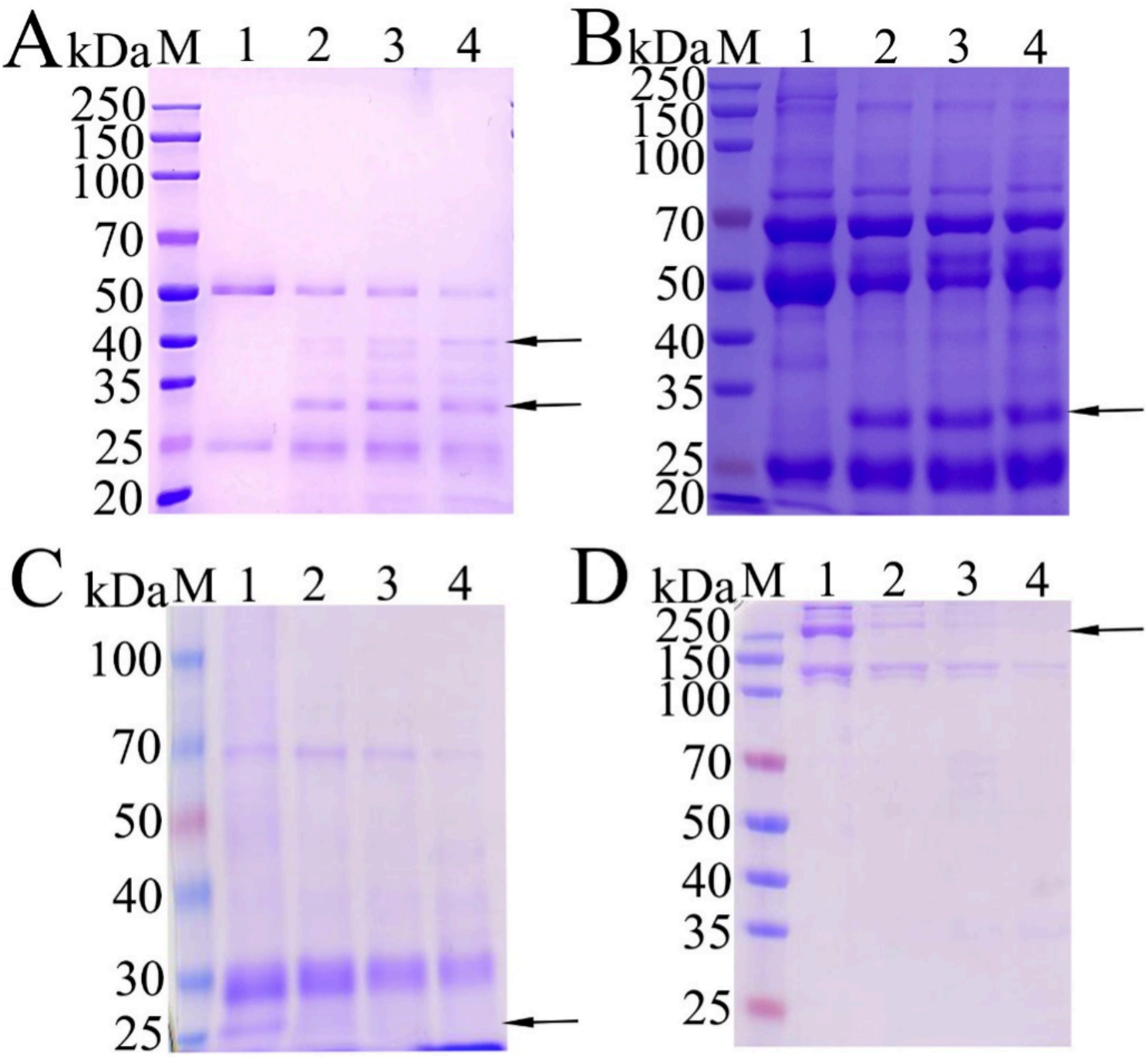


Figure 6

SDS-PAGE analysis of substrate degradation by rTsATG4B.

A-D Degradation profiles of human IgG, goat IgG, mouse hemoglobin and rat tail type I collagen, respectively. Lane M: protein molecular weight marker; Lane 1: substrate only; Lanes 2-4: substrate co-incubated with 1, 2, 3 μg rTsATG4B, respectively.

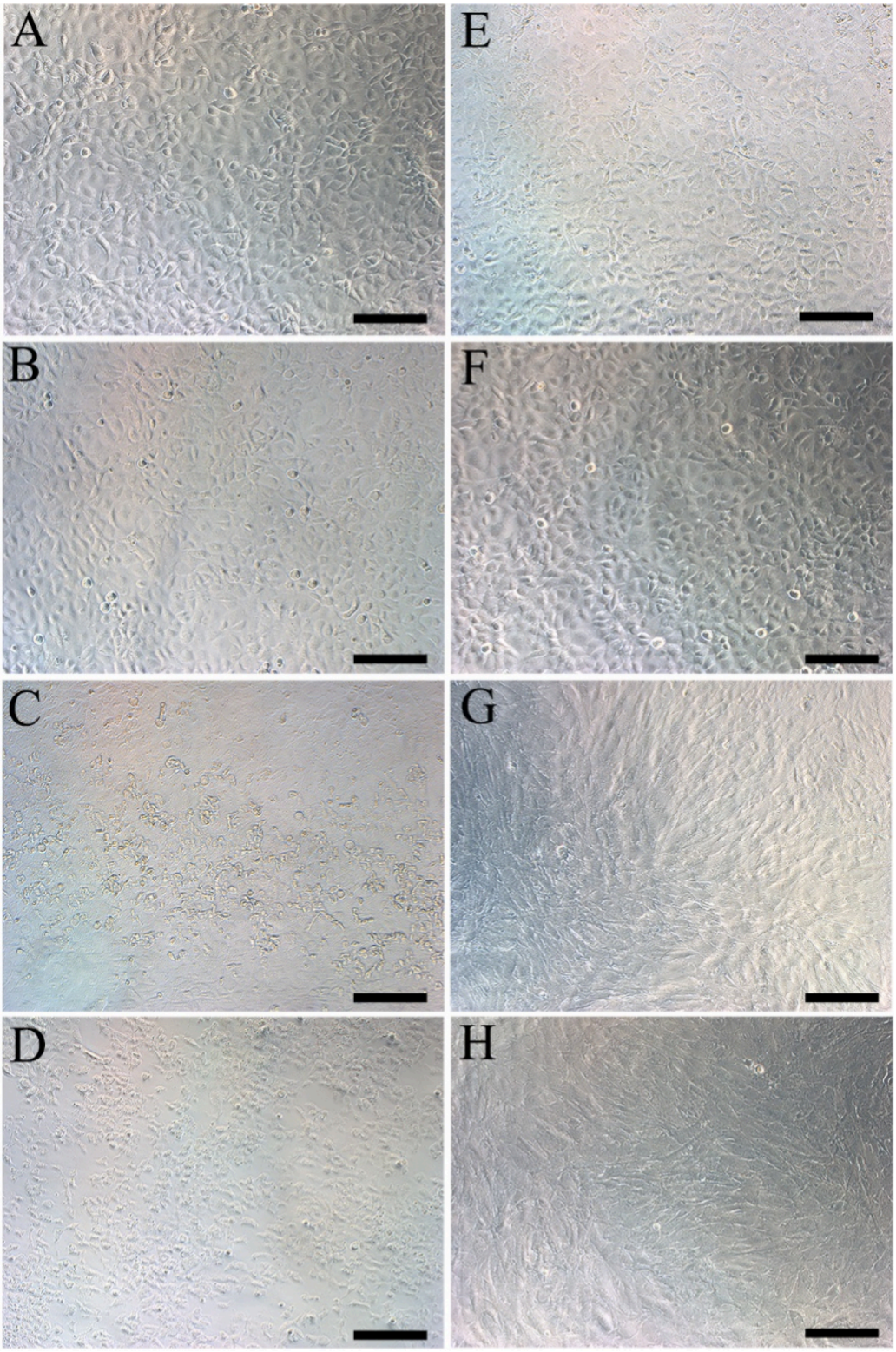


Figure 7

Morphological damage of primary mouse intestinal epithelial cells (IECs) induced by rTsATG4B.

A PBS blank control; **B-D** IEC monolayers treated with 12 μg/mL rTsATG4B for 30, 60 and 120 min, respectively; **E** E-64 preincubation group (protease activity blocked, no cell injury); **F** Papain positive

control group; **G**rTsATG4B-treated C2C12 myoblasts; **H** PBS-treated C2C12 myoblasts. Scale bar=100 μm.

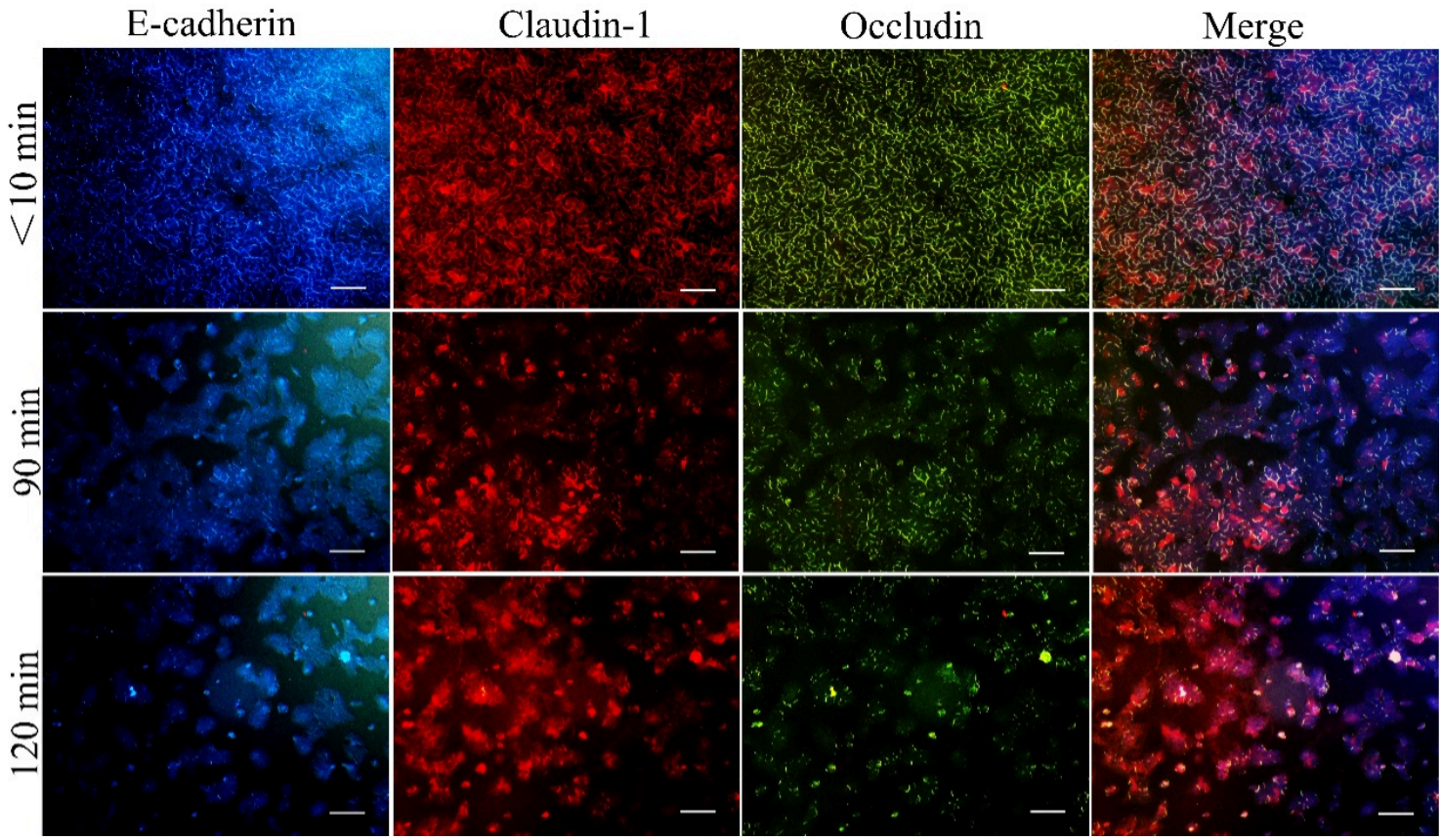


Figure 8

Immunofluorescence detection of disrupted intercellular tight junction proteins in HT29 monolayers treated with rTsATG4B.

HT29 cells were incubated with 12 μg/mL rTsATG4B for 10, 90 and 120 min, followed by immunostaining for E-cadherin, claudin-1 and occludin. Scale bar=100 μm.

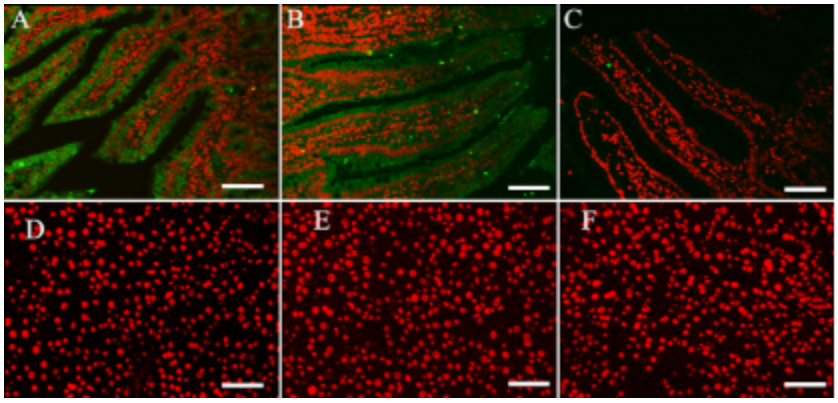


Figure 9

IIFT for specific binding of rTsATG4B to normal mouse small intestinal epithelium.

A-C Small intestinal tissue sections incubated with anti-rTsATG4B immune serum, *T. spiralis*-infected mouse serum and preimmune serum, respectively. **D-F** Liver tissue sections incubated with the three types of serum above as negative tissue control. Cell nuclei were counterstained with PI. Scale bar=100 μm.

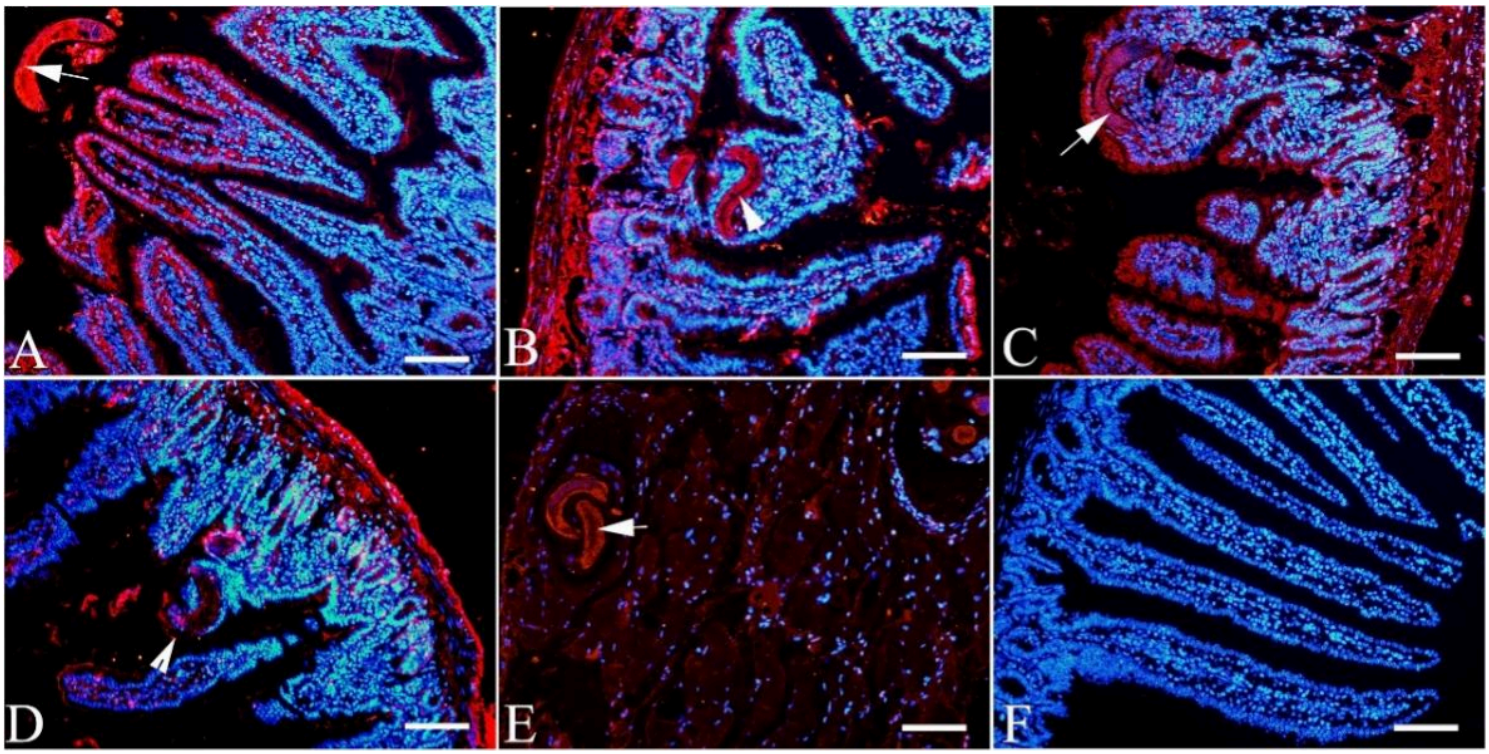


Figure 10

***In vivo* IIFT localization of native TsATG4B and mucosal pathological lesions during *T. spiralis* larval infection.**

A-D Small intestinal villi collected at 2, 6, 8 and 12 h post-infection (hpi); **E** Diaphragm muscle tissues at 42 days post-infection (dpi) as tissue control; **F**Small intestine from uninfected normal mice. Scale bar=100 μm.

Supplementary Files

This is a list of supplementary files associated with this preprint. Click to download.

- ThecysteineproteaseATG4B.pdf